



Published in final edited form as:

Nat Methods. 2017 April ; 14(4): 331–332. doi:10.1038/nmeth.4193.

MotionCor2 - anisotropic correction of beam-induced motion for improved cryo-electron microscopy

Shawn Q. Zheng^{1,2}, Eugene Palovcak¹, Jean-Paul Armache¹, Kliment A. Verba¹, Yifan Cheng^{1,2}, and David A. Agard^{1,2}

¹Department of Biochemistry and Biophysics, University of California, San Francisco, California 94143, USA

²Howard Hughes Medical Institute, University of California, San Francisco, California 94143, USA

In recent years single-particle cryo-electron microscopy (cryo-EM) has made groundbreaking advancements in obtaining atomic resolution structures of macromolecules^{1,2}. Central to this success has been the broad application of direct electron detection cameras having high output frame rates, enabling recording images of frozen hydrated biological samples as dose-fractionated stacks of sub-frames (movies). Beam-induced sample motion that blurs the captured images can then be corrected by registering identical features in the sub-frames, followed by summing the registered sub-frames to produce a motion-corrected image³.

Beam-induced sample motion can be decomposed into two components, uniform whole frame motion and non-uniform local motions that are idiosyncratic and varying across the image. We previously developed an algorithm⁴, implemented in the program MotionCorr, that made use of redundant measurements of image shifts between all sub-frames to derive a least squares estimate of relative motions between neighboring sub-frames. It provided an efficient correction of whole frame image motions with sufficient accuracy for determination of near atomic resolution 3D reconstructions⁵. A different algorithm, assuming that particles located nearby have similar trajectories, tracks individual particle motion as part of 3D refinement^{6,7}. A commonly used strategy nowadays is to correct whole frame motion first in raw micrographs and track particle motions towards the end of the refinement of final reconstructions.

Here we develop an algorithm based on an experimentally validated model that describes the sample motion as a local deformation that varies smoothly throughout the exposure. Tilting experiments show that the non-uniform motions seen in movie stacks are projections of complex 3D sample deformations onto the image plane (Figure 1a). We use a time-varying

Correspondence should be addressed to: Y.C. (ycheng@ucsf.edu) or D.A.A. (agard@msg.ucsf.edu).

Author Contributions:

S.Q.Z. implemented the algorithm and wrote all codes for MotionCor2. D.A.A. contributed to algorithm development, S.Q.Z., E.P., Y.C., D.A.A. designed experiments to evaluate the performance of MotionCor2. K.A.V. designed initial experiments for camera defect correction. S.Q.Z. and E.P. carried out image processing. E.P. and J.P.A. collected low-defocus cryo-EM images of 20S proteasomes. S.Q.Z., E.P., Y.C. and D.A.A. wrote the manuscript. All authors participated in discussion and revision of the manuscript.

Competing Financial Interests:

The authors declare no competing financial interest.

two-dimensional (2D) polynomial function to describe these projections. The image is first divided into patches and motions within each patch are iteratively determined. The resultant shifts are used to fit the 2D polynomial functions that smoothly vary with time. Each image sub-frame is subsequently remapped using this smooth polynomial function at each individual pixel (Figure 1b) and summed with or without radiation damage weighting. This algorithm is implemented as MotionCor2, a program running on Linux using multiple GPUs. It combines the correction of both uniform whole frame motion and anisotropic local motion, and streamlines all the necessary preprocessing steps including bad pixel detection/correction, prior to the normal cryo-EM processing pipeline (Supplementary Figure 2 and 3).

We tested the performance of MotionCor2 using two previously acquired single particle cryo-EM datasets: the archaeal 20S proteasome⁴ and the rat TRPV1 ion channel⁵ and compared the results with the results with MotionCorr. MotionCor2 significantly improves high-resolution Thon ring signals and leads to better correlation with simulated contrast transfer functions (Supplementary Figure 4). 3D reconstructions of the 20S proteasome were determined from images that were motion-corrected by MotionCorr, Unblur⁸ and MotionCor2, followed by refinement and reconstruction with RELION (Figure 1c). Using MotionCorr and Unblur with dose weighting but without further particle polishing, we obtained 3D reconstruction of 2.7(6)Å and 2.6(9)Å nominal resolutions. Using Unblur followed by particle polishing improved the resolution to 2.5(7)Å. Using MotionCor2 with dose weighting, we obtained a 3D reconstruction of 2.5(0)Å resolution, comparable to combining Unblur with particle polishing. We also tested applying the RELION per-frame B-factor weighting scheme instead of dose weighting, but with MotionCor2-determined shifts. This resulted in a slightly improved nominal resolution of 2.4(6)Å, which was almost identical to the reconstruction obtained from using particle polishing after MotionCor2 correction. This suggests that further tracking individual particle trajectories after local motion correction by MotionCor2 provides minimal, if any, improvement in resolution, and that further improvements in the dose-weighting scheme may be possible.

Similarly, we re-processed our previous raw micrographs from the TRPV1 ion channel and re-determined its 3D reconstruction improving the resolution from 3.5Å to 3.1(5)Å (Supplementary Figure 5). The improvements are particularly obvious in some trans-membrane regions, where extra densities associated with the TRPV1 protein are now seen to have well-defined features that can only now be interpreted as lipid molecules. We also tested that MotionCor2 enabled motion correction on images recorded with low defocus at 200kV again with superior results (Supplementary Figure 6 and 7).

Lastly, we tested the performance of MotionCor2 on movie stacks of a tomographic tilt series collected from frozen hydrated *Drosophila* centrioles, where a particle tracking strategy is not applicable. Again, a comparison was made between MotionCor2 and Unblur in terms of restoring Thon rings of tilted images using the cross correlation metrics from CTFFIND4. The results show that local motion correction substantially improved Thon rings of every tilt image in this tomographic tilt series (Supplementary Figure 8).

Overall, MotionCor2 is extremely robust, and sufficiently accurate at correcting local motions so that the very time-consuming and computationally-intensive particle polishing in RELION can be skipped. Importantly, it also works on a wide range of data sets including cryo tomographic tilt series.

Methods

Methods, additional experiments and any associated references are available in the online version of the paper.

Data Availability

The pre-compiled program MotionCor2 can be downloaded for academic use as Supplementary Software. Latest updates can be found in <http://msg.ucsf.edu/em/software/index.html>.

Supplementary Material

Refer to Web version on PubMed Central for supplementary material.

Acknowledgments

We thank X. Li for helpful discussion during the initial stage of this work. We also thank M. Braunfeld for supporting the cryo-EM facility at UCSF, G. Greenan for providing his cryo tomographic tilt series collected on a *Drosophila* centriole, and C. Kennedy for supporting the computational infrastructure for processing cryo-EM data. This work was supported in part by grants from National Institute of Health, R01GM031627 to D.A. and P01GM111126, P50GM082250, R01GM082893 and R01GM098672 to Y.C. Y.C. and D.A. are Investigators of Howard Hughes Medical Institute.

References

1. Cheng Y. Single-Particle Cryo-EM at Crystallographic Resolution. *Cell*. 2015; 161:450–457. DOI: 10.1016/j.cell.2015.03.049 [PubMed: 25910205]
2. Kuhlbrandt W. Biochemistry. The resolution revolution. *Science*. 2014; 343:1443–1444. DOI: 10.1126/science.1251652 [PubMed: 24675944]
3. Brilot AF, et al. Beam-induced motion of vitrified specimen on holey carbon film. *J Struct Biol*. 2012; 177:630–637. DOI: 10.1016/j.jsb.2012.02.003 [PubMed: 22366277]
4. Li X, et al. Electron counting and beam-induced motion correction enable near-atomic-resolution single-particle cryo-EM. *Nature Methods*. 2013; 10:584–590. [PubMed: 23644547]
5. Liao M, Cao E, Julius D, Cheng Y. Structure of the TRPV1 ion channel determined by electron cryo-microscopy. *Nature*. 2013; 504:107–112. DOI: 10.1038/nature12822 [PubMed: 24305160]
6. Bai XC, Fernandez IS, McMullan G, Scheres SH. Ribosome structures to near-atomic resolution from thirty thousand cryo-EM particles. *eLife*. 2013; 2:e00461. [PubMed: 23427024]
7. Rubinstein JL, Brubaker MA. Alignment of cryo-EM movies of individual particles by optimization of image translations. *J Struct Biol*. 2015; 192:188–195. DOI: 10.1016/j.jsb.2015.08.007 [PubMed: 26296328]
8. Grant T, Grigorieff N. Measuring the optimal exposure for single particle cryo-EM using a 2.6 reconstruction of rotavirus VP6. *eLife*. 2015; 4

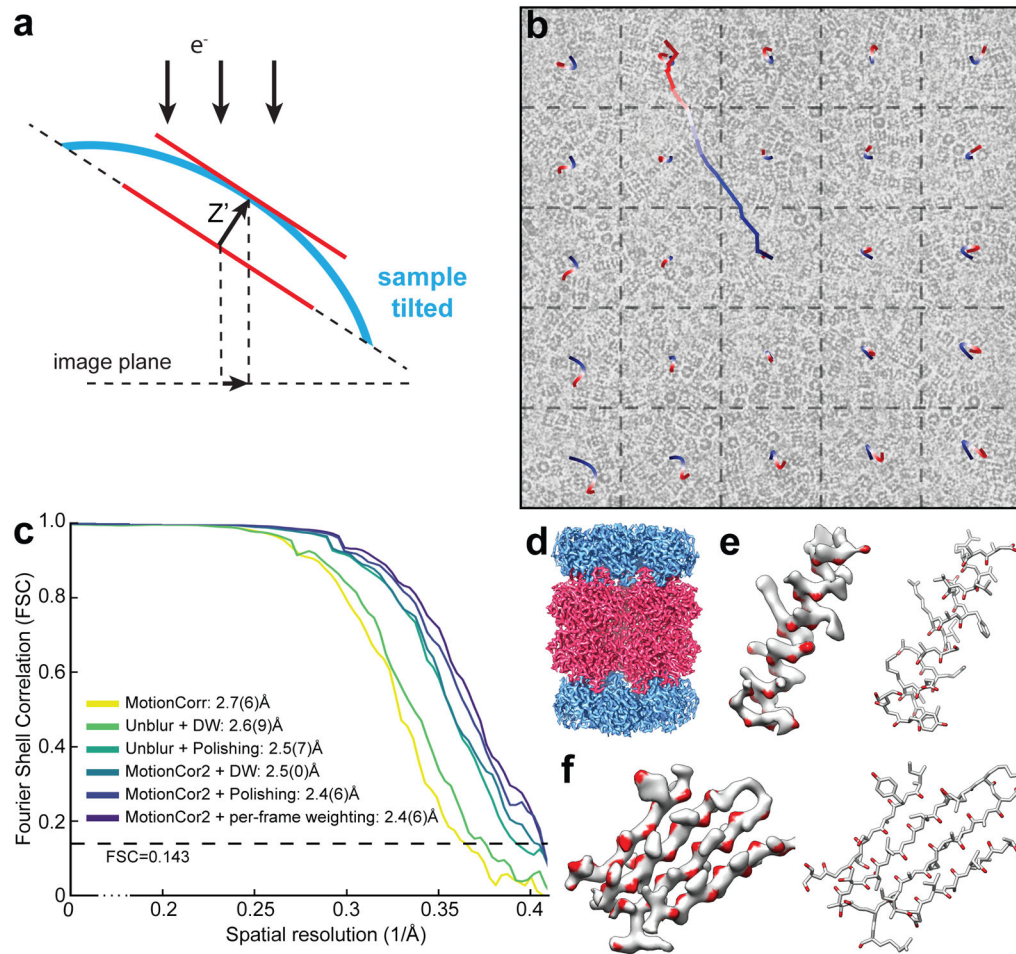


Figure 1. Local motion correction by MotionCor2

(a) Schematic drawing illustrates that, when the sample is tilted, the observable motions in the image plan is the projection of z-motion produced by doming of the sample under electron beam. (b) Image of frozen hydrated archaeal 20S proteasome overlaid with the traces of global motion based upon whole frame alignment (long trace originated from the center of image) and each patch predicted from the polynomial function. (c) Fourier Shell Correlation (FSC) curves of 3D reconstructions determined using micrographs corrected by Unblur with dose weighting, Unblur followed by particle polishing, correction by MotionCor2 with dose-weighting, MotionCor2 followed by particle polishing and MotionCor2 with per-frame B-factor weighting. The color code is marked in the figure. (d) 3D reconstruction of archaeal 20S proteasome filtered to 2.5 \AA resolution and sharpened by a temperature factor of -103.8\AA^2 . (e) Density of a β -sheet, where the main chain carbonyl is colored in red. Visualization of main chain carbonyl density requires better a resolution that is better than 3 \AA . (f) Representative side chain densities.